WEP Warwick Evans Publishing

Transactions on Engineering and Technology Research
ISSN: 2960-1797, eISSN: 2960-2246 | Volume 6
MECEME 2026

Construction of Dynamic Water Flow Propagation Models for Mine Water Inrushes and Research on Time-Dependent Evacuation Path Optimization

Zhanxiang Jiang [1], Pengyun Yan [2], Yupeng Zhang [2], Yunfan Yang [3, *]

[1] School of Environmental and Chemical Engineering, Hebei Vocational University of Industry and Technology, Shijiazhuang, China

[2] School of Artificial Intelligence, Hebei Vocational University of Industry and Technology, Shijiazhuang, China,

[3] Department of Basic Education, Hebei Vocational University of Industry and Technology, Shijiazhuang, China

* Corresponding Author Email: jjzxxy@outlook.com

Abstract. Mine water disasters pose significant safety challenges to mining operations, often resulting in substantial casualties and property losses. This study focuses on two key issues following mine water inrushes: modeling the propagation patterns of water flow (dynamic propagation modeling for single-point water inrushes) and optimizing personnel escape routes (optimizing optimal escape paths for miners during water inrush scenarios). First, based on rectangular roadway cross-section characteristics and unidirectional water flow propagation rules, we calculate roadway lengths using Euclidean distance and employ a breadth-first search (BFS) algorithm to construct a water flow propagation model. This precisely quantifies the arrival times of water at each endpoint and the roadway's complete flooding time. Second, under dynamic flow constraints (e.g., water level, passage time window, and personnel movement speed), miner escape path planning is abstracted as a shortest path problem with dynamic constraints. Employing a time-dependent Dijkstra algorithm, we dynamically update the cumulative shortest escape time for each node, successfully planning optimal escape routes for miners and obtaining shortest escape time results across different elevation scenarios. This study provides a scientific quantitative analysis method and escape decision support for emergency response to mine water disasters.In order to deal with the mine flood, which is a major potential safety hazard, reduce casualties and property losses.

Keywords: BFS algorithm; time-dependent Dijkstra algorithm; Euclidean distance calculation.

1. Introduction

Mine flooding, ranking as the foremost of the five major hazards in safe mining operations, is characterized by its sudden onset and severe consequences. Once triggered, it readily causes significant casualties and property damage. Due to complex hydrogeological conditions and other factors, mine tunnel systems typically form a three-dimensional network structure with intersecting passages, further complicating flood prevention and emergency response [1]. When a water inrush accident occurs, rapidly and accurately simulating the propagation process of the water flow is the core prerequisite for formulating scientific rescue plans and planning safe escape routes. This study focuses on a scenario where water propagates forward at a constant rate of 30m³/min within a rectangular cross-section tunnel (4m wide, 3m high). Based on this context, this paper proposes and solves two core problems. First, modeling the dynamic propagation of water flow from a single inflow point: A model must be established for the flow propagation of the water surge within the tunnel. Given the conditions, the water flow propagates unidirectionally only horizontally and downward through the tunnel, with branching not altering its velocity. By analyzing the water propagation process, the arrival times of the water flow at each tunnel endpoint and the time of complete flooding for each tunnel are calculated[2-3]. Second, it addresses the optimization of optimal escape routes for miners during a water inrush scenario: Based on the aforementioned water propagation results, it

plans the optimal escape routes for miners under the constraint of an evacuation notice issued one minute after the water inrush[4]. To address the dynamic flow propagation modeling for a single water inrush point, this paper first calculates tunnel lengths using Euclidean distances based on endpoint 3D coordinates[5]. Subsequently, a breadth-first search (BFS) algorithm constructs the flow propagation model to traverse flow paths, thereby computing endpoint arrival times and tunnel flooding times. To solve the miner optimal escape path optimization problem in water inrush scenarios, this paper builds upon the water propagation results. It incorporates dynamic constraints such as tunnel passage time windows, water level height, and personnel movement speed to construct a dynamic constraint path optimization model. The solution employs a time-dependent Dijkstra algorithm, which continuously updates the cumulative shortest escape time for each node. Ultimately, the optimal escape path is obtained through backtracking [6-7].

2. Model Establishment and Solution

2.1. Model Establishment

Based on the physical characteristics of mine water inrush, a physical model for water flow propagation was constructed [8]:

Tunnel Simplification

All tunnels were simplified as standard rectangular sections with a width of 4 m and a height of 3 m, where the bottom edge of the section is parallel to the horizontal plane.

Water Flow Characteristics

The initial water level of the inrushing water was 0.1 m, and the water inrush volume was constant at $30\ \mathrm{m}^3/\mathrm{min}$.

Propagation Rules

Water flow only spreads to horizontal and downward tunnels. At branch nodes, the flow is evenly distributed, and the initial water level remains unchanged after distribution.

To accurately match the two key stages of water flow propagation and correspond to the two core output indicators required in Problem 1 (water arrival time at endpoints, tunnel full time), and to ensure that the model calculation is highly consistent with the physical process and problem requirements, two volume stages were introduced: the initial water level stage (corresponding to V_0) and the full water level stage (corresponding to V_1). When water first reaches a tunnel, it needs to fill up to the initial water level of 0.1 m (as specified in the problem, "the height that can be maintained after water first arrives"). The water volume required for this stage is V_0; when V_0 is filled, it indicates that the water has covered the tunnel bottom and reached the endpoint at the other end of the tunnel for the first time. After the initial water level is formed, water continues to be injected, rising from 0.1 m to the top of the 3 m-high tunnel (fully filled). The additional water volume required for this stage is $\mathrm{V}_1 - \mathrm{V}_0$, and the total water volume required is V_1; when V_1 is filled, the tunnel is completely submerged. This directly corresponds to the definition of "tunnel full time". Using a single volume would confuse the essential difference between "partial filling" and "complete filling", leading to errors in time calculation [9-10].

From the problem, the following formulas are derived:

$$V_0 = acL_1 \tag{1}$$

$$V_1 = abL_i \tag{2}$$

Impact of Tunnel Elevation Characteristics on Water Flow Propagation

A distinction was made between the scenario with uniform elevation (Scenario 1) and the scenario with varying elevations (Scenario 2) in the dataset. Given that all tunnels in Scenario 1 have the same elevation (no height difference), water flow propagation is not affected by differences in gravitational potential energy. In Scenario 2, tunnels have elevation differences (different c values), so water flow only spreads to horizontal or downward tunnels.

Time parameter calculation required the introduction of an "elevation constraint", and the two scenarios were analyzed separately:

(1) Scenario 1 (Uniform Elevation)

The calculation depends on the "full time of the previous tunnel". In horizontal tunnels, water can only advance after the upstream tunnel is completely filled, which conforms to the static water propagation characteristics when there is no height difference.

Since the tunnel elevations in Scenario 1 are the same, the influence of the z-axis was ignored to reduce computational complexity. The Euclidean distance formula was used to calculate the tunnel length:

$$L = \sqrt{(x_2 - x_1)^2 + (y_2 - y_1)^2} \tag{3}$$

The calculated tunnel lengths are shown in Figure 1:

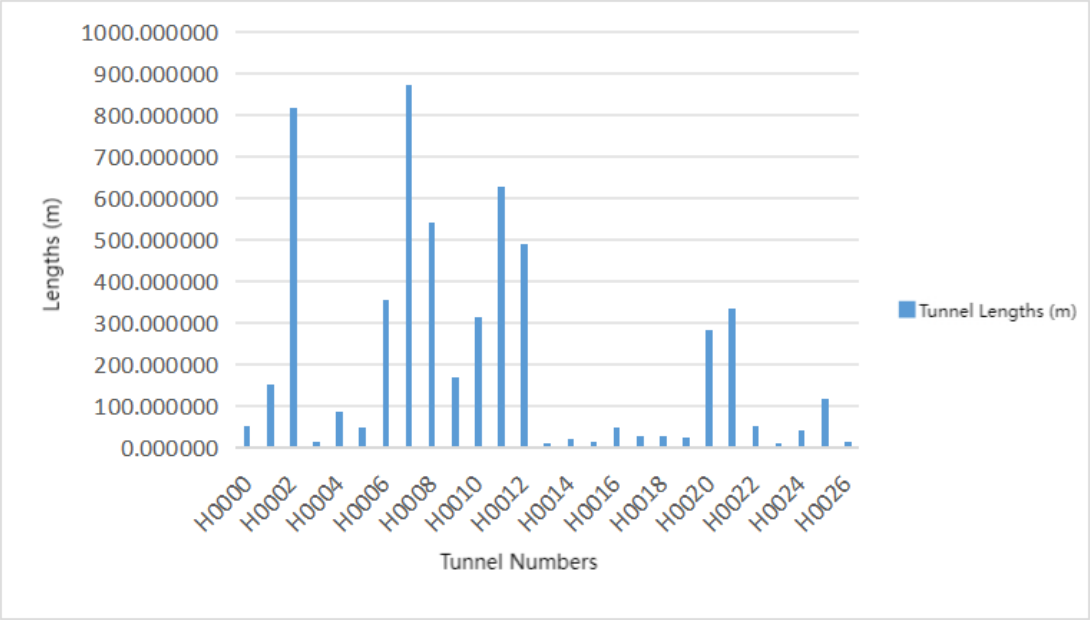

Figure 1. Tunnel Lengths in Scenario 1

To intuitively display the tunnel connection relationship and the location of the water inrush point, and given the uniform elevation in Scenario 1, the following diagram (Figure 2) was generated:

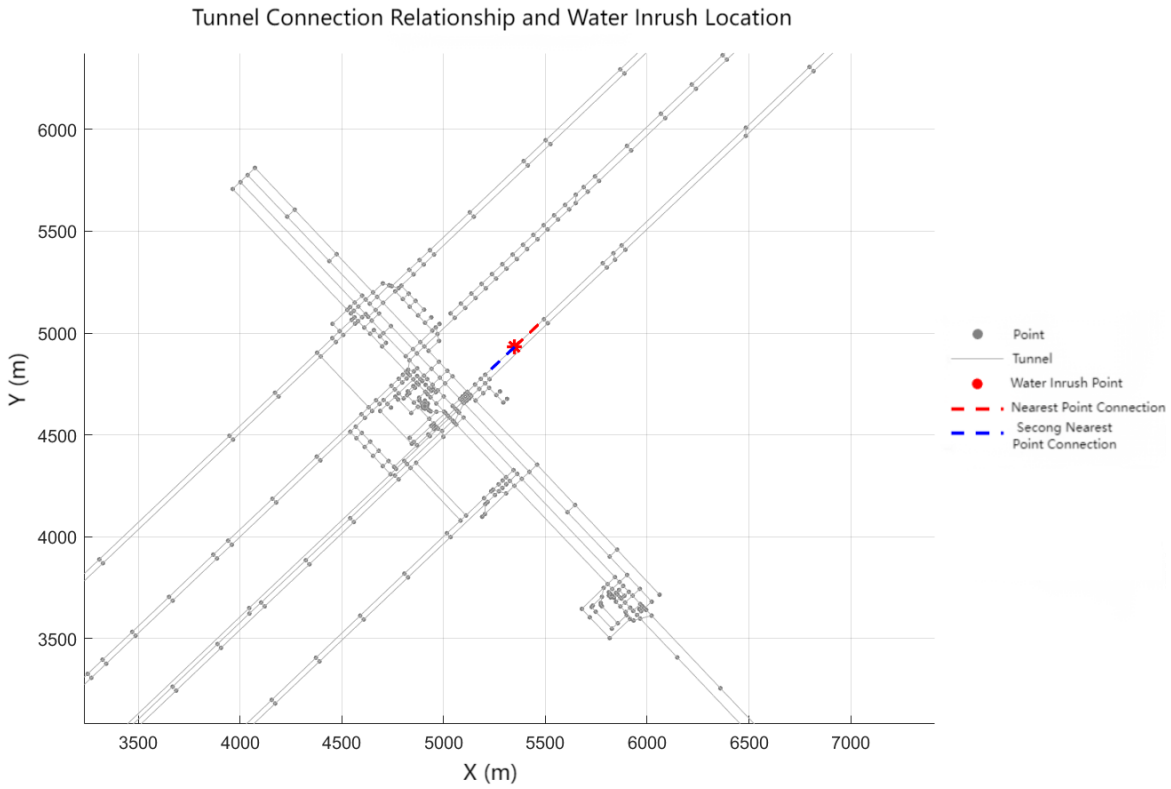

Figure 2. Tunnel Connection Relationship and Water Inrush Point Location in Scenario 1

Water Arrival Time at Endpoints:

$$t_{a,i} = t_{f,i-1} + 0.1 \times 4 \times \frac{L_i}{Q} \tag{4}$$

Tunnel Full Time:

$$t_{f,i} = t_{f,i-1} + 3 \times 4 \times \frac{L_i}{Q} \tag{5}$$

The final calculated results are shown in Figures 3 and 4 below:

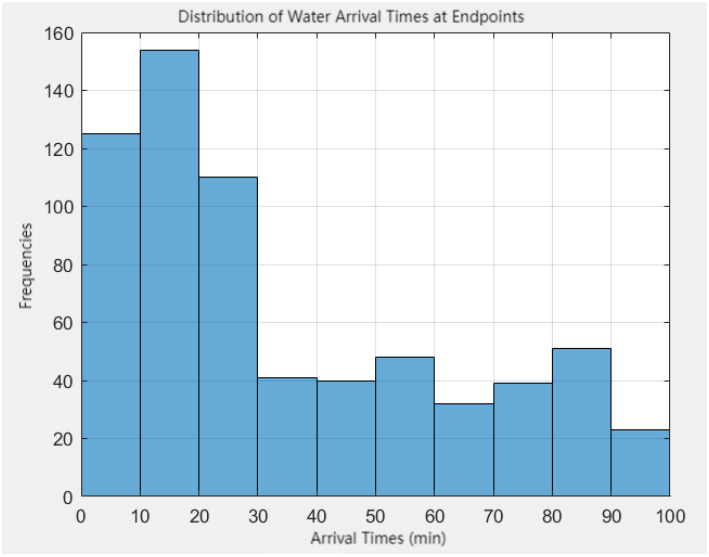

Figure 3. Distribution of Water Arrival Times at Endpoints in Scenario 1

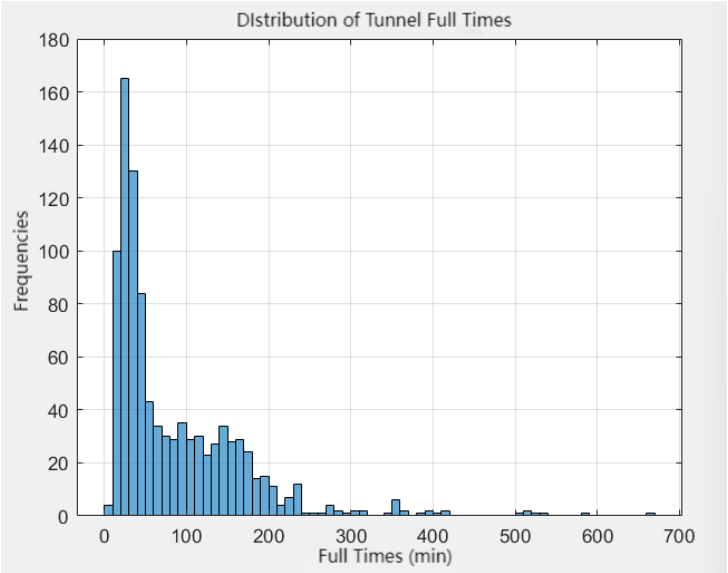

Figure 4. Distribution of Tunnel Full Times in Scenario 1

(2) Scenario 2 (Varying Elevations)

The calculation depends on the condition that "elevation ≥ full time of the current upstream tunnel". In downward tunnels, water flow is driven by gravity and only spreads from fully filled tunnels at higher elevations.

Tunnel Length Calculation for Scenario 2:

$$L = \sqrt{(x_2 - x_1)^2 + (y_2 - y_1)^2 + (z_2 - z_1)^2} \tag{6}$$

Partial tunnel lengths are shown in the Table 1:

Table 1. Partial Tunnel Lengths in Scenario 2

Tunnel No.	H0002	H0003	H0004	H0005	H0006	H0007	H0008	H0009	H0010
Endpoint 1	P0003	P0005	P0005	P0005	P0005	P0010	P0011	P0012	P0014
Endpoint 2	P0004	P0006	P0007	P0008	P0009	P0011	P0012	P0013	P0015
Length (m)	817.473217	15.205295	87.948995	49.366802	356.194202	873.604329	540.899787	170.727652	315.08271

Since the variation in the z-axis is much smaller than that in the x and y axes, the effect is shown in Figure 5; therefore, the scale was adjusted to obtain Figure 6 for easier observation:

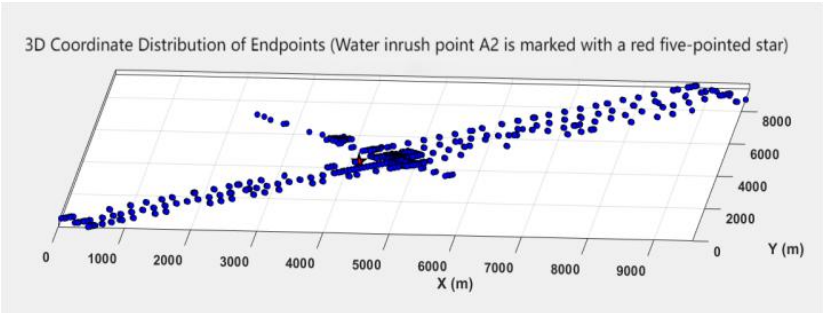

Figure 5. 3D Coordinate Distribution of Endpoints

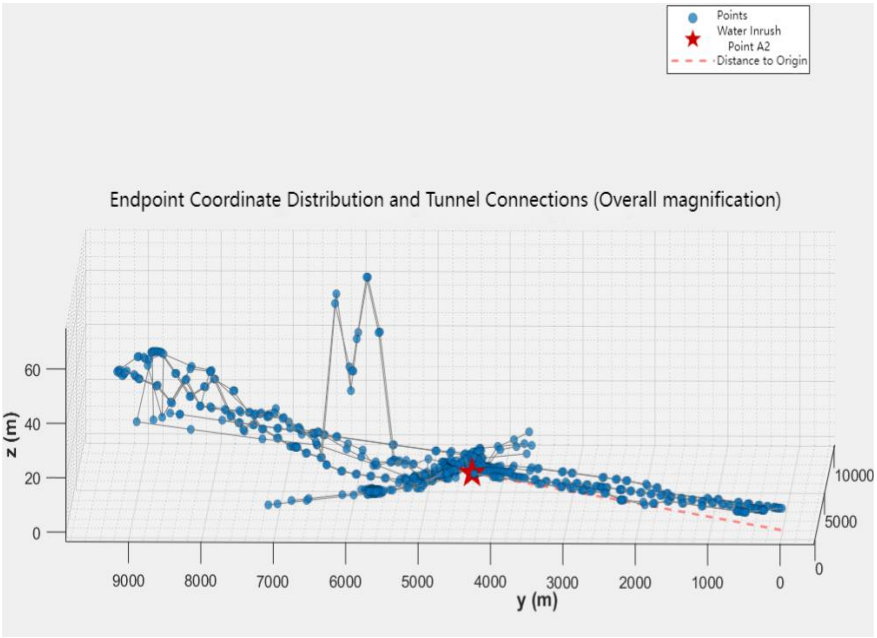

Figure 6. Endpoint Coordinate Distribution and Tunnel Connections

Tunnel Full Time:

$$t_{f,i} = t_{f,j} + 3 \times 4 \times \frac{L_i}{Q} \tag{7}$$

Water Arrival Time at Endpoints:

$$t_{a,i} = t_{f,i} + 0.1 \times 4 \times \frac{L_i}{Q} \tag{8}$$

The final calculated results are shown in Figures 7 and 8 below:

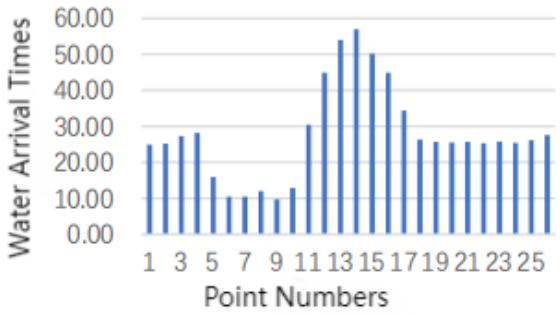

Figure 7. Water Arrival Times at Endpoints in Scenario 2

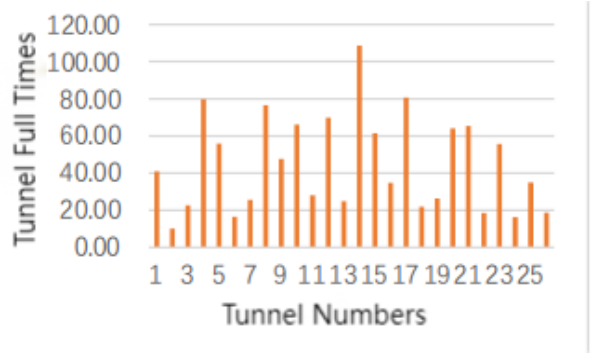

Figure 8. Tunnel Full Times in Scenario 2

2.2. Model Solution

Based on the given parameters (rectangular section with a width of 4 m and a height of 3 m, initial water level of 0.1 m for inrushing water) and data from the dataset, the model results were obtained using MATLAB (see the appendix for the program; results are stored in the files result1-1.xlsx and result1-2.xlsx).

3. Model Establishment and Solution

3.1. Model Establishment

Taking the miners' escape paths (a sequence consisting of a series of tunnels and endpoints) as the core decision-making object, and under the premise that the escape start time is fixed (1 minute after water inrush) following a mine water inrush, the feasibility of escape paths was analyzed based on the different relationships between water flow propagation laws and personnel movement rules. By comparing feasible paths, the optimal path that minimizes the total escape time for miners was determined.

The maximum allowable water surface height for tunnel passage was denoted as $h_m = 0.3$ m, and the tunnel full time was denoted as t_f. Miners were labeled as Miner 1, Miner 2, and Miner 3 in the given order. From Problem 1 and the problem settings, the following conclusions were drawn:

For any Tunnel i with endpoints m and n, where the water arrival time at endpoint m is $t_{a,m}$ and at endpoint n is $t_{a,n}$, the criterion for determining that Tunnel i is not covered by water is that the current time $t < \max(t_{a,m}, t_{a,n})$; the tunnel full time $t_{f,i}$ of Tunnel i is calculated.

General Relationship Between Escape Path Feasibility, Path Parameters, and Water Flow Status

In the mine tunnel network coordinate system, the miners' initial positions and exit positions can be mapped to tunnel endpoints or virtual nodes. Although there may be time errors in water flow propagation (the actual calculation is based on an ideal model, and no errors can be assumed), the positional error of miners' horizontal movement is negligible (assuming miners can move accurately along tunnels). The water flow status in tunnels (whether water has arrived, water surface height) can be determined from the results of Problem 1 and is deterministic. For any Tunnel i, the formula for calculating the water surface height $h_i(t)$ in Tunnel i at time t is:

$$h_i(t) = \frac{Q \times max(0, t - t_{a,j})}{L_i \times S_i} \tag{9}$$

where $t_{a,i} = \max(t_{a,m}, t_{a,n})$ is the time when water arrives at Tunnel i.

Based on the different relationships between $h_i(t)$ and h_m, between the time when miners enter Tunnel i (t_{in}) and $t_{f,i}$, and between the water flow direction and the miners' escape direction, tunnel passage conditions were classified into the following categories for analysis:

Category I: Excessive water surface height, passage prohibited;

Category II: Water surface height not excessive, but outside the tunnel full time window, passage prohibited;

Category III: Water surface height not excessive and within the time window, no water flow, passage at the no-water speed;

Category IV: Water surface height not excessive and within the time window, water flow exists and is in the same direction as escape, passage at the downstream speed;

Category V: Water surface height not excessive and within the time window, water flow exists and is opposite to escape, passage at the upstream speed.

3.2. Scenario-Specific Solution Strategy for Escape Paths

This problem is a time-dependent shortest path problem with dynamic constraints. The core requirement is to "plan the shortest-time path for miners from their initial positions to exits under the dynamic constraints of water flow propagation". Since constraints (time window, water surface height, speed) change dynamically with time and location, and it is necessary to handle two types of scenarios—"planar with no elevation" and "three-dimensional with elevation"—the improved time-dependent Dijkstra algorithm was selected as the basic framework, with customized extensions for different scenarios. The specific improvements are shown in Table 2 below:

Table 2. Comparison of Improvements to the Dijkstra Algorithm

Standard Dijkstra Algorithm	Improved Time-Dependent Dijkstra Algorithm (Planar Scenario)	Improved Time-Dependent Dijkstra Algorithm (3D Scenario with Elevation)
Initialize node distances to infinity, starting node distance to 0	Initialize cumulative node time to infinity, set starting node time to 60 seconds	Initialize cumulative node time to infinity, set starting node time to 60 seconds, and synchronously record node elevation
Construct static edge weights (fixed distance)	Construct dynamic edge weight functions (time-dependent travel time)	Construct dynamic edge weight functions (time + elevation-dependent travel time)
Select the node with the smallest distance from the priority queue	Select the node with the smallest cumulative time from the priority queue	Select the node with the smallest cumulative time from the priority queue (with additional elevation safety scoring)
Traverse neighboring nodes and calculate new distances	Traverse neighboring nodes and calculate the time t_{in} when entering the tunnel	Traverse neighboring nodes, calculate the time t_{in} when entering the tunnel, and obtain the elevations of the two ends of the tunnel
Update if the new distance is smaller	1. Calculate water flow arrival status to determine speed; 2. Verify water surface height constraints; 3. Verify time window constraints; 4. Calculate and update new cumulative time if all constraints are satisfied	1. Correct water flow direction based on elevation; 2. Calculate speed after slope correction; 3. Verify basic constraints + low-elevation safety redundancy; 4. Calculate and update new cumulative time if all constraints are satisfied
Repeat steps 3–5 until reaching the destination	Repeat steps 3–5 until all exit nodes are visited	Repeat steps 3–5 until all exit nodes are visited
Output the shortest path	Output the shortest-time path that satisfies constraints	Output the shortest-time path that satisfies constraints (with attached elevation change curve)

(1) Path Feasibility Analysis for the Planar Scenario (No Tunnel Elevation Difference)

In the planar scenario, all tunnels are horizontal with no elevation difference. The water flow direction is only determined by the water arrival time at endpoints, and speed constraints are only related to the water flow direction:

Category I: Excessive water surface height, passage prohibited. When $h_i(t) > h_m$, the water surface height in the tunnel exceeds the allowable value, posing a drowning risk, so the tunnel cannot be part of the escape path;

Category II: Water surface height not excessive, but outside the time window, passage prohibited. If $h_i(t) \le h_m$, but the time when miners enter Tunnel i (t_{in}) satisfies $t_{in} + L_i/v > t_{f,i}$ (where v is

the corresponding speed), it means the tunnel will be filled with water during passage, so passage is prohibited;

Category III: No water flow and within the time window, passage at 240 m/min. When $t < t_{a,i}$ (i.e., $h_i(t) = 0 < h_m$) and $t_{in} + L_i/4 \leq t_{f,i}$, there is no water flow in the tunnel, and miners pass at a speed of 240 m/min;

Category IV: Water flow exists in the same direction as escape and within the time window, passage at 120 m/min. When $t \geq t_{a,i}$ (with $h_i(t) \leq h_m$), $t_{in} + L_i/2 \leq t_{f,i}$, and the miners' escape direction is consistent with the water flow direction (from the endpoint reached earlier to the endpoint reached later), miners pass at a speed of 2 m/s;

Category V: Water flow exists opposite to escape and within the time window, passage at 60 m/min. When $t \geq t_{a,i}$ (with $h_i(t) \leq h_m$), $t_{in} + L_i/1 \leq t_{f,i}$, and the miners' escape direction is opposite to the water flow direction, miners pass at a speed of 60 m/min.

The escape routes of the three miners were visualized using MATLAB, as shown in Figures 9, 10, and 11 below:

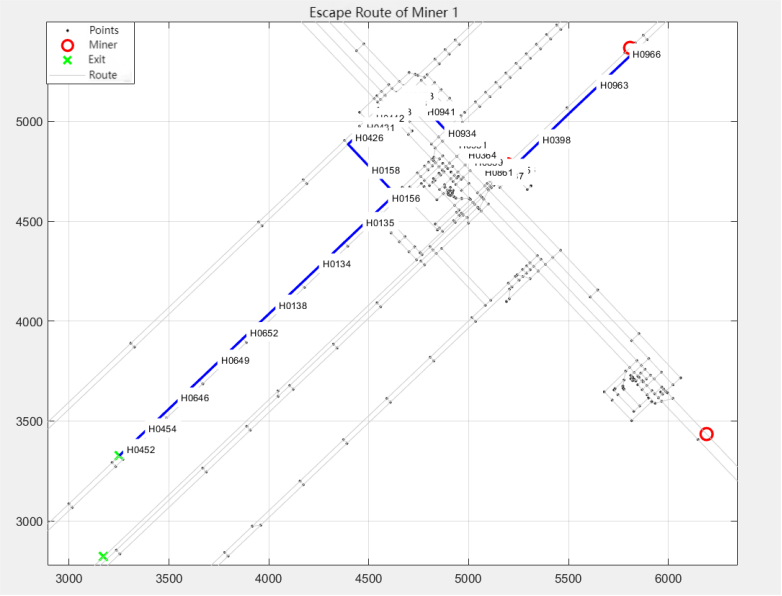

Figure 9. Escape Route of Miner 1

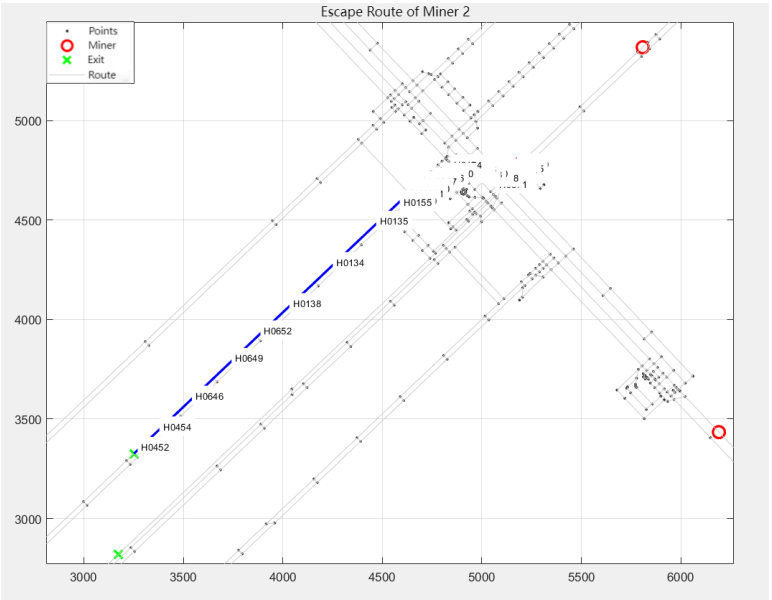

Figure 10. Escape Route of Miner 2

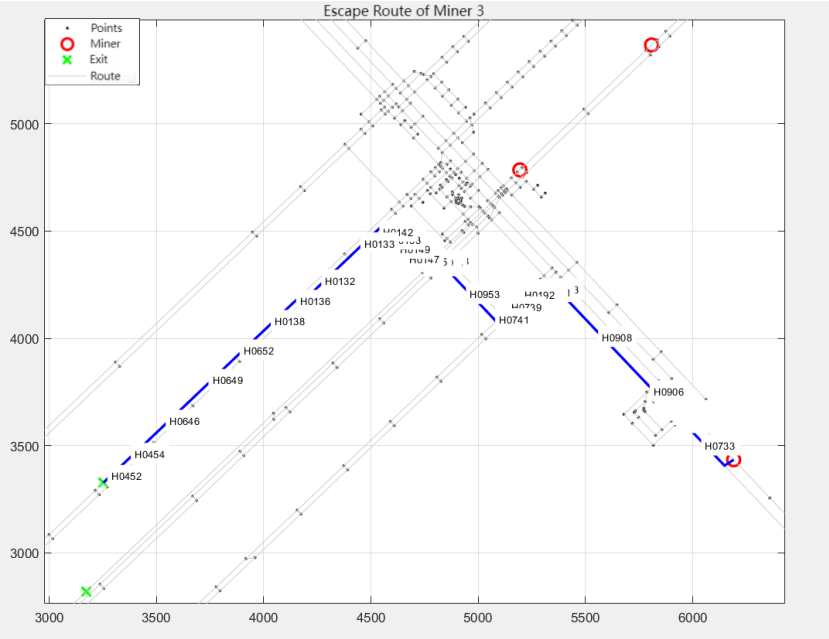

Figure 11. Escape Route of Miner 3

Based on the above analysis and solution, the optimal escape times for the three miners in the planar scenario were approximately 1389.82 s, 737.87 s, and 1089.02 s.

(2) Path Feasibility Analysis for the 3D Scenario (With Tunnel Elevation Difference)

In the 3D scenario, tunnels have elevation differences (the elevations of endpoints are denoted as c_m and c_n). The water flow direction is dominated by gravity, and speed constraints need to incorporate the impact of elevation on movement:

Category I: Excessive water surface height, passage prohibited. The judgment logic is consistent with the planar scenario: when $h_i(t) > h_m$, the tunnel is impassable;

Category II: Water surface height not excessive, but outside the time window or at low-elevation risk, passage prohibited. Basic constraint: If $h_i(t) \le h_m$ but $t_{in} + L_i/v' > t_{f,i}$ (where v' is the speed corrected for elevation), passage is prohibited. Additional constraint: For tunnels with elevation lower than a certain threshold (e.g., the elevation of the lowest exit), even if the time window constraint is satisfied, it is necessary to verify that $t_{f,i} \ge t_{in} + 60$ (reserving a 60-second safety buffer); otherwise, passage is prohibited due to the high risk of submersion in low-elevation areas;

Category III: No water flow and within the time window, speed affected by elevation. Downslope (escape direction consistent with the direction of elevation decrease): speed is corrected to 240β m/min ($\beta \ge 1$, e.g., 1.1 for downslope assistance); upslope (escape direction consistent with the direction of elevation increase): speed is corrected to 240α m/min ($\alpha < 1$, e.g., 0.8 for upslope resistance); horizontal sections: passage still at 240 m/min;

Category IV: Water flow exists in the same direction as escape and within the time window, speed affected by both elevation and water flow direction. Water flow direction consistent with the direction of elevation decrease (downslope and downstream): speed is corrected to 120β m/min; water flow direction consistent with the direction of elevation increase (upslope and downstream): speed is corrected to 120α m/min; it is necessary to simultaneously satisfy $t_{in} + L_i/v' \le t_{f,i}$;

Category V: Water flow exists opposite to escape and within the time window, speed affected by both elevation and water flow direction. Water flow direction consistent with the direction of elevation decrease (downslope and upstream): speed is corrected to 1α m/s (upstream resistance partially offset by downslope); water flow direction consistent with the direction of elevation increase (upslope

and upstream): speed is corrected to $1\alpha^2$ m/s (superimposed resistance from upstream and upslope); it is necessary to simultaneously satisfy $t_{in} + L_i/v' \leq t_{f,i}$.

The escape routes of the three miners were visualized using MATLAB, as shown in Figures 12, 13, and 14 below:

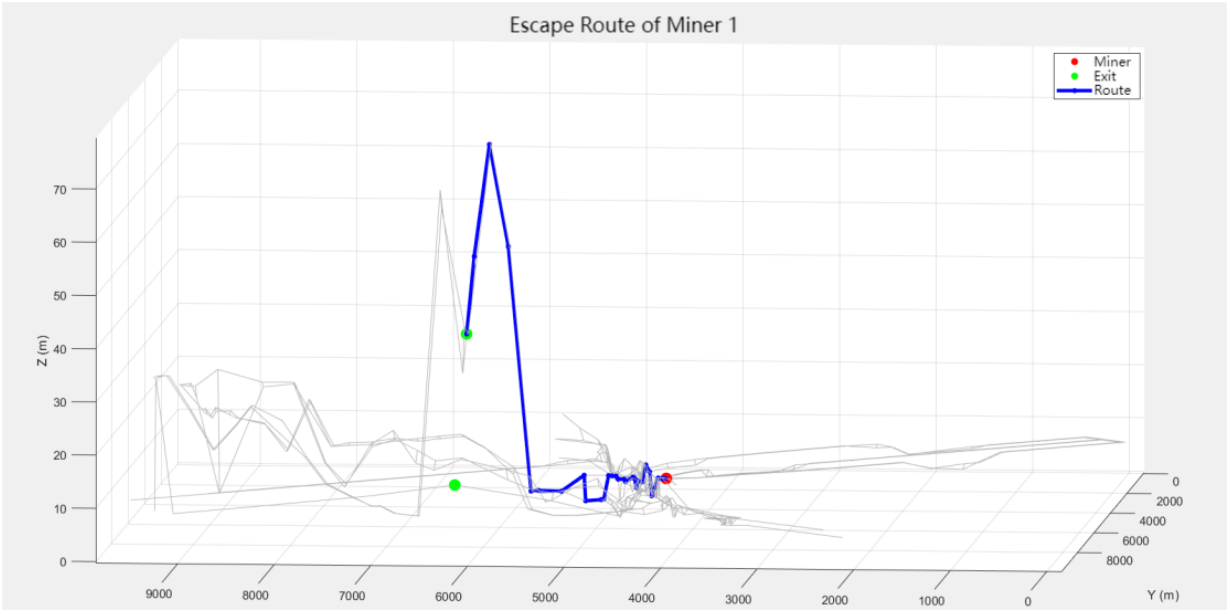

Figure 12. Escape Route of Miner 1

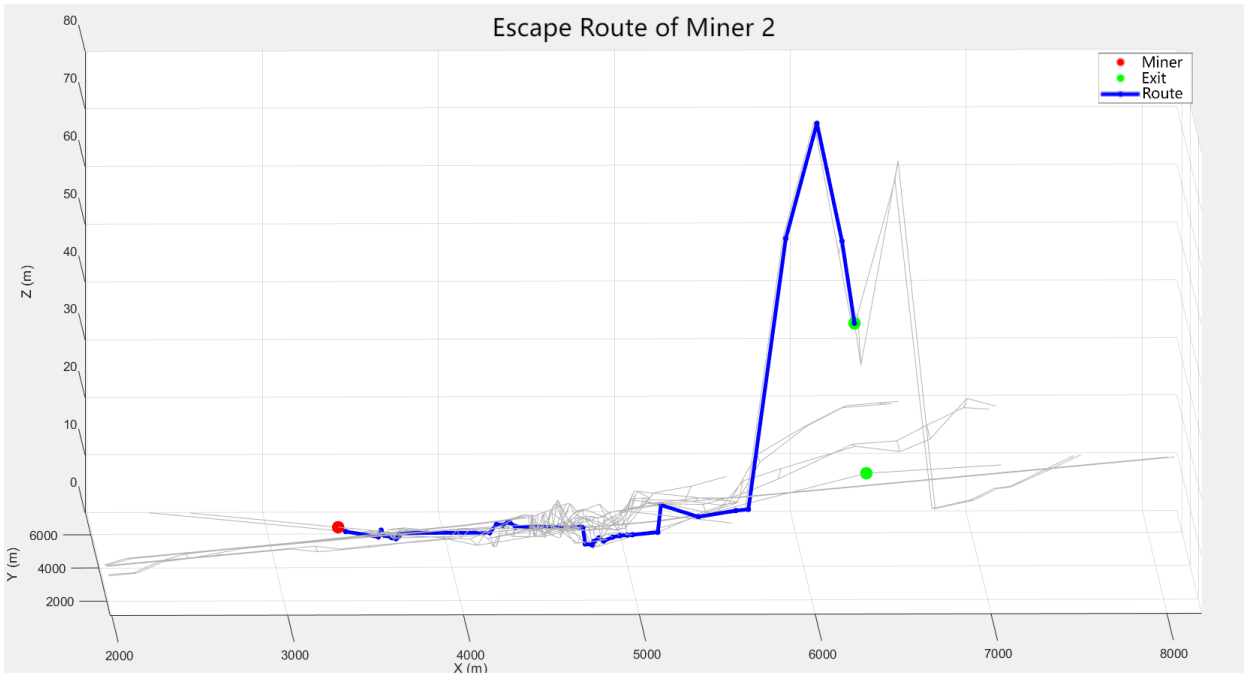

Figure 13. Escape Route of Miner 2

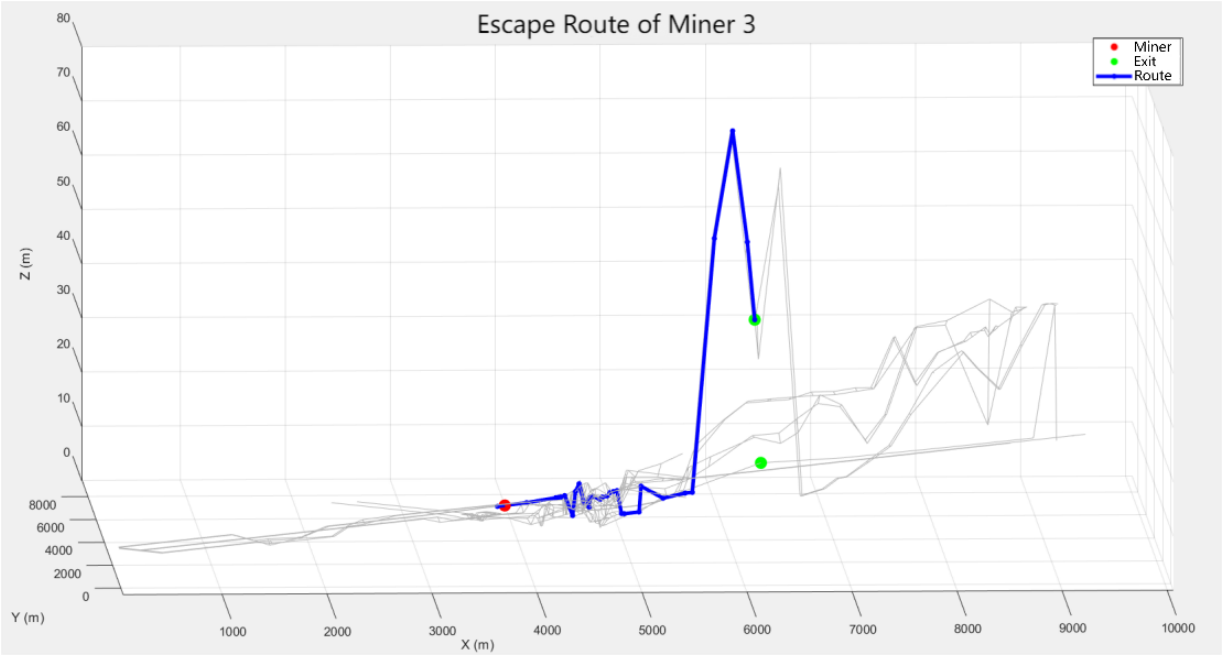

Figure 14. Escape Route of Miner 3

Based on the above analysis and solution, the optimal escape times for the three miners in the 3D scenario were approximately 682.16 s, 1028.52 s, and 880.96 s.

4. Conclusions

This paper successfully constructs a dynamic water flow propagation model for single-point water inrush scenarios. It utilizes Euclidean distance to calculate roadway length and combines the BFS algorithm to precisely determine the water arrival times at each endpoint and the roadway flooding time. Building upon this foundation, the model incorporates dynamic constraints such as passage time windows, water level height, and personnel movement speed to optimize the miner's escape path. Employing a time-dependent Dijkstra algorithm, this study identifies the shortest escape time path for miners within the dataset. In the future, it can be extended to mine emergency rescue training system and build a simulation experimental platform for mine water inrush escape.

References

[1] Zhang Yang. Research on Fire Source Detection and Escape Route Optimization Algorithm Based on Improved YOLOv8 and Genetic Algorithm [D]. Inner Mongolia University of Science and Technology, 2025.

[2] Li Wei, Zhang Chuan, Yuan Jian, et al. Research on Optimized Escape Device Design for Pressure-Operated Gas Well Machines [J]. C
DOI: CNKI: SUN: SBGL.0.2024-21-047.

[3] Li Ying, Zhao Ningxi. Optimization Algorithm and Implementation of Shortest Escape Paths in Ship Interiors Based on B/S Architecture [J]. Surveying and Mapping Geoinformation, 2024, 49(04): 24-30. DOI: 10.14188/j.2095-6045.2022727.

[4] Lu Guoju, Gao Caijun. Research on Mine Shortest Escape Path Planning Based on an Improved Gray Wolf Optimization Algorithm [J]. Metal Mines, 2024, (03): 244-248.

[5] Ni Huilin, Wang Hongnan, Ning Yuan, et al. Optimization Plan and Numerical Simulation Analysis of Escape Facilities in University Dormitories [J]. Industrial Safety and Environmental Protection, 2023, 49(10): 20-23.

[6] Yang Lin, Liu Zhuojun, Shi Lingxia. Structural Optimization Study of Emergency Escape Passages on a Ro-Ro Passenger Ship [J]. Guangzhou Shipyard Technology, 2023,43(02):4-8.

[7] Fan Ye. Research on Safety Evacuation Optimization for Underground Commercial Streets Based on VR Escape Experiments [D]. Zhengzhou University, 2023.

[8] Zhang Zhilong, Fu Jingjie. Optimized Design of Emergency Escape Door Control Circuit for Urban Rail Transit Trains Based on FMECA Technology [J]. Railway Technology Supervision, 2022, 50(07): 39-41+45.

[9] Chen Juntao. Research and Development of Intelligent Early Warning Device for Ship Capsizing Escape and Its Applicability Optimization [J]. China Water Transport (Lower Half-Month), 2021, 21(08): 5-6.

[10] Du Baojiang, Lin Laishuai, Tang Qiang, et al. Optimization of Virtual Fire Escape Paths Based on Ant Colony Optimization Algorithm [J]. Software Guide, 2018, 17(04): 71-76+81.